CAVITATION DAMAGE AND CORRELATIONS WITH MATERIAL AND FLUID PROPERTIES

R. Garcia
F. G. Hammitt

The University of Michigan

Department of Nuclear Engineering

Laboratory for Fluid Flow and Heat Transport Phenomena

Internal Report 05031-11-I

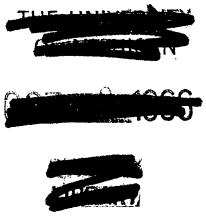

Financial Support Provided By

NATIONAL SCIENCE FOUNDATION
(Grant G-22529)

September, 1966

ABSTRACT

A comprehensive set of cavitation damage data has been obtained in a vibratory facility using water, mercury, lithium, and lead-bismuth alloy as test fluids, and covering temperatures ranging from room temperature to 1500°F. Materials tested include a wide variety of metals and alloys. From this data a simple, reasonably precise, damage predicting equation has been derived, including only ultimate resilience as a material property, but also corrections for cavitation "thermodynamic effects" and NPSH. It has been found that of the conventional mechanical properties, ultimate resilience is the most successful in this regard.

A direct comparison between venturi and vibratory cavitation damage shows that the relative rankings of materials remains about the same for mercury, and a good correlation is obtained between the mercury data from the venturi and ultimate resilience. Neither statement applies for the water venturi data, possibly because of the greater effects of corrosion in the low intensity cavitation field.

ACKNOWLEDGMENTS

The authors would like to acknowledge the financial support of the National Science Foundation which provided support for this work. Mechanical properties data supplied by Pratt & Whitney Aircraft (CANEL) and The University of Michigan Department of Chemical & Metallurgical Engineering is also gratefully appreciated.

Special thanks are also due Dr. Clarence A. Siebert, Professor of Chemical & Metallurgical Engineering; Dr. M. John Robinson, Lecturer in Nuclear Engineering; Mr. Richard L. Crandall, Research Assistant, Computing Center; and Mr. Allen R. Schaedel, Research Assistant in the Department of Nuclear Engineering; all of The University of Michigan, for many helpful suggestions and continuing interest in this project.

TABLE OF CONTENTS

LIST OF TABLES

LIST OF FIGURES

Figure Page

CAVITATION DAMAGE AND CORRELATIONS WITH MATERIAL AND FLUID PROPERTIES

I. INTRODUCTION

For the past two hundred years the phenomenon of cavitation has been known, and the accompanying losses of component performance and material damage have been of considerable concern to the designers of fluid machinery since the turn of the century. In the earliest considerations of the cavitation phenomenon the primary fluid of interest was water. At the present, however, liquid metals, cryogenics, organics, and other fluids have also come into prime consideration as heat transfer media and working fluids in thermodynamic cycles in space, nuclear, and other more conventional systems. For all of these applications it becomes necessary to know realistically under what conditions cavitation can be anticipated, and the quantity and quality of damage to be expected for a given degree of cavitation, since it may not be possible or desirable to avoid the cavitating regime entirely by overconservative design, as has often been the past practice for conventional applications. Thus, the laboratory testing of various materials to determine their cavitation damage resistance becomes important. Experimental facilities for this purpose may be grouped into two categories: those that depend on inducing low pressures as a result of velocity

changes in flowing liquids, and those using an acoustic field in a static liquid to induce cavitation.

In our laboratory we have used both types: a venturi system and a vibratory unit. While a flowing system such as a venturi presumably models field conditions fairly closely, the time and cost of its operation are relatively high, so that the simpler, faster, and more economical vibratory test is often preferred. In the present investigation the same fluids and temperatures have been used in both facilities to some extent. Thus, a direct comparison of cavitation resistance of various materials in these two types of facilities is available. Such direct comparisons for a wide variety of materials have not in general been available in the past. .

Data from the present experiments covers a very wide spectrum of materials, fluids, and temperatures, particularly in the vibratory device. Hence, correlating relations, which must of necessity include material, fluid, and flow parameters, have been examined in an attempt to generate a reasonably simple relation, based as much as possible on physical reasoning, to allow the à priori estimation of damage in a similar facility, but with different materials, fluids, temperatures, etc. This has, indeed, been accomplished.

The fluids tested in this program include lead-bismuth alloy, mercury, water, and lithium. Since the results from the tests on the first three fluids have already been reported,[1,2,3,4] only the lithium tests and results are discussed herein.

II. EXPERIMENTAL EQUIPMENT

The high-temperature vibratory facility and the venturi facilities in this laboratory have been described elsewhere.[4,5] Since the present paper deals mainly with the vibratory facility, a brief summarization of its major features is included. As shown in Figure 1, it consists of an audio-oscillator, power-amplifier, transducer-horn assembly, test specimen, oscilloscope, frequency counter, high-temperature furnace, cavitation vessel, and accelerometer (attached to the top of the horn for amplitude measurement). The signal supplied by the variable-frequency audio-oscillator is amplified and applied to the piezoelectric crystals. Their periodic motion generates a standing wave whose amplitude is increased as it traverses the exponential horn assembly, to which the test specimens are attached at the small end. For high-temperature tests the transducer-horn assembly is installed in the special cavitation vessel which is filled with the appropriate fluid and inserted in an electric furnace. Argon is used as cover gas above the fluid. Figure 2 is a photograph of the facility showing the horn assembly installed in the cavitation vessel, which in turn is inserted into the furnace.

Figure 3 shows the test specimen design. Dimensions "A" and "B" vary with material density to maintain uniform weight for all specimens.

The facility has been operated successfully with various fluids at temperatures up to 1500°F at a frequency of $\sim$20 Kc./sec. and double amplitude of $\sim$ 2 mils.

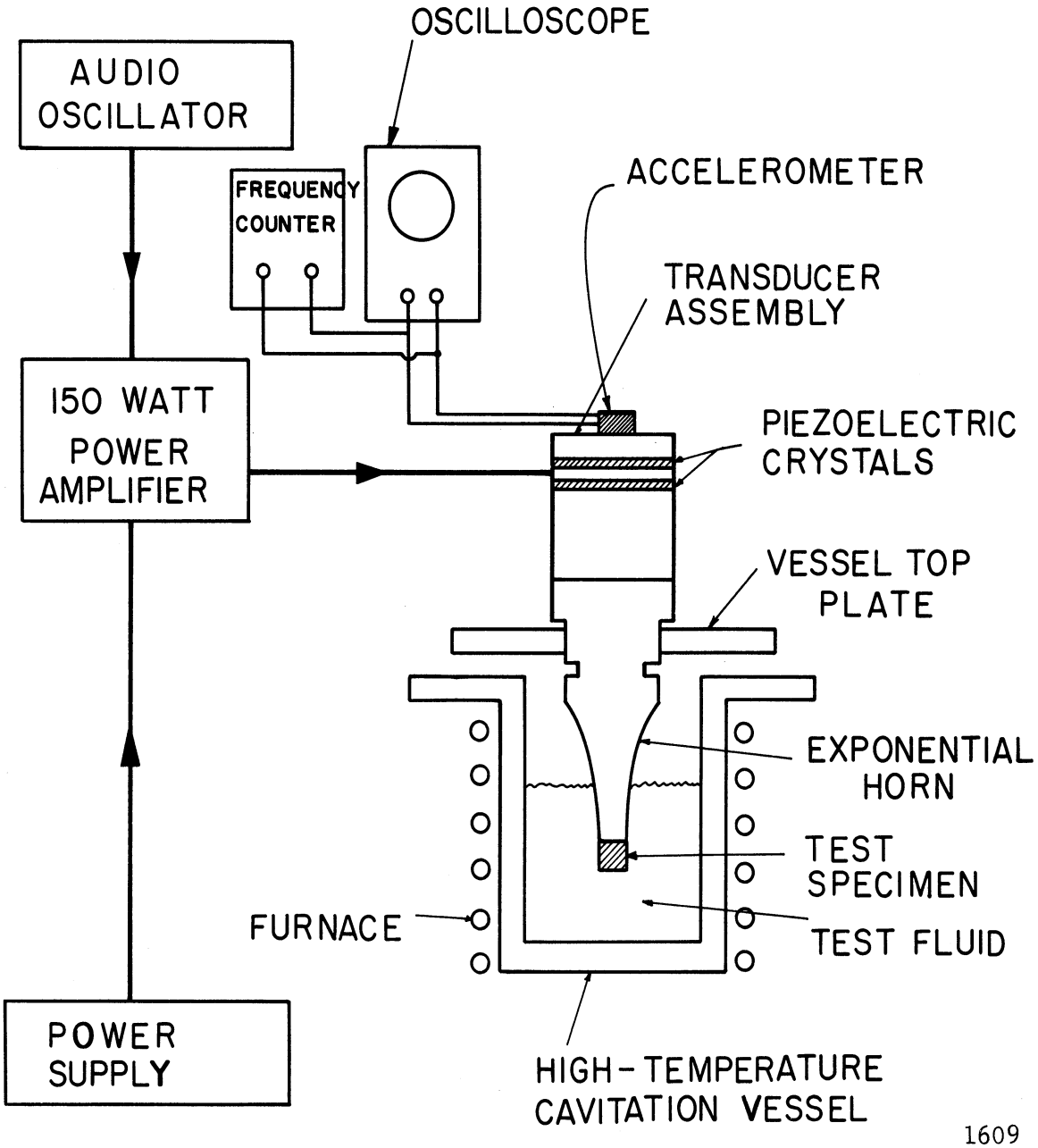

Fig. 1.--Schematic block diagram of the high-temperature ultrasonic vibratory facility.

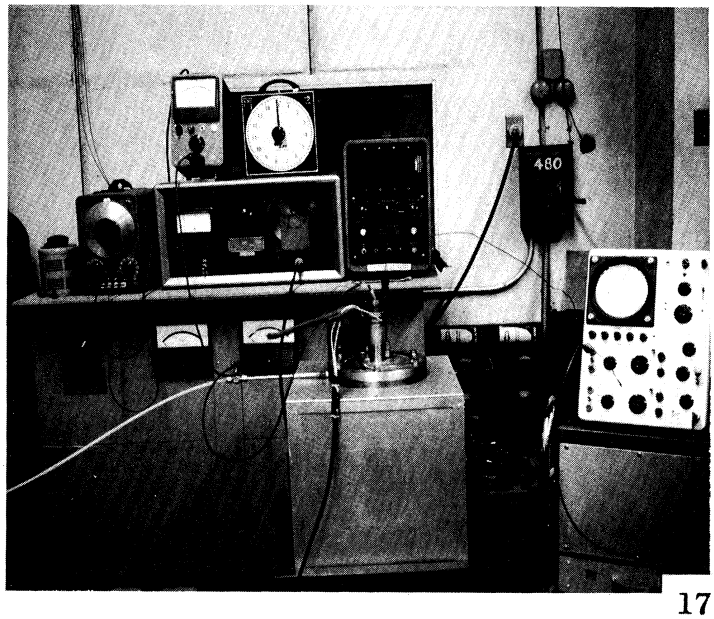

Fig. 2.--Photograph of the high-temperature cavitation facility.

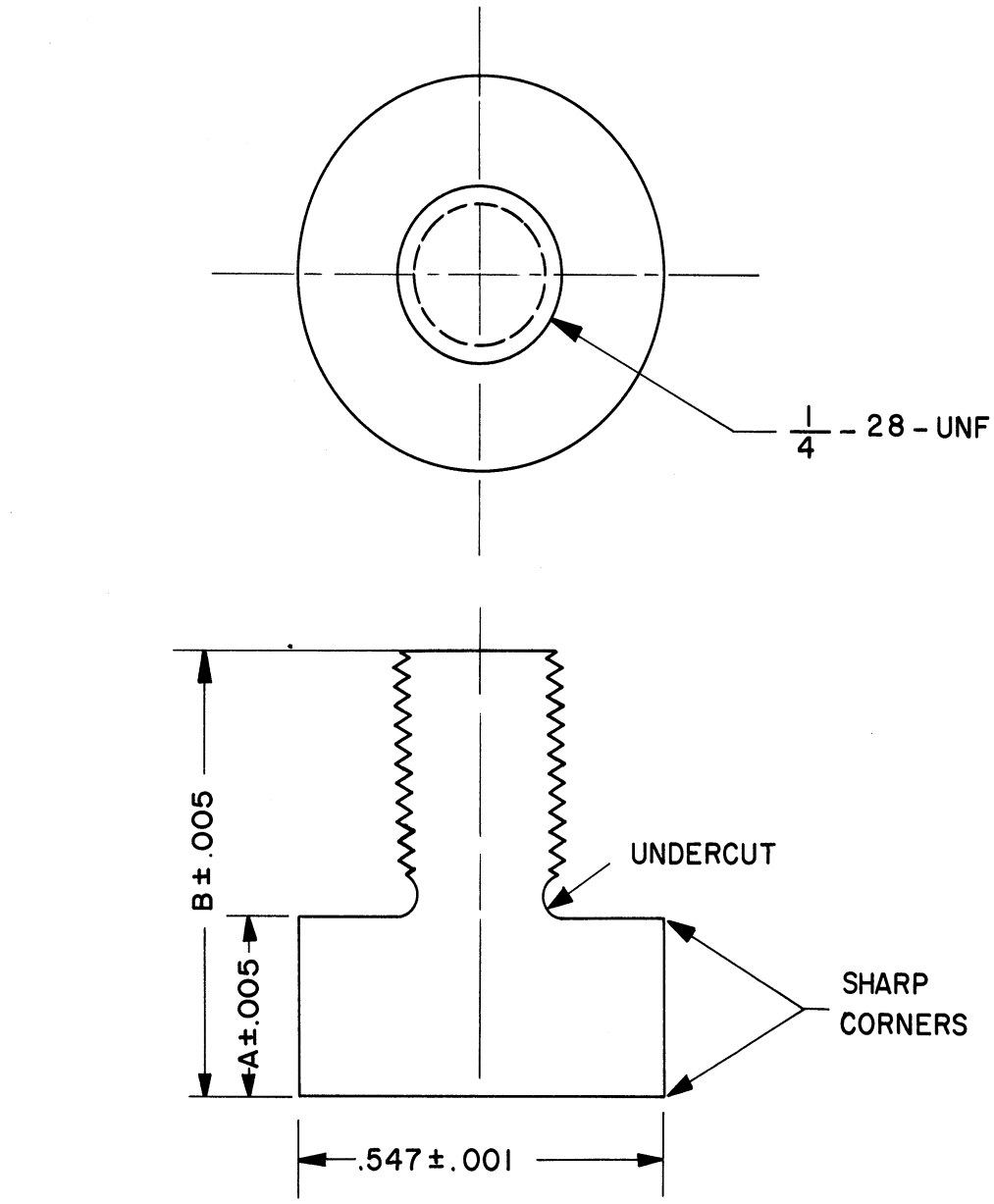

Fig. 3.--Standard cavitation test specimen.

III. EXPERIMENTAL INVESTIGATIONS

A. General. It was desired to determine the cavitation resistance of a wide variety of potentially useful materials, involving as broad a range of mechanical properties as possible in a wide variety of fluids and over a large temperature range in order to learn more about the cavitation damage process as it is affected by fluid and material properties. Tests in some of the same fluids with the same materials were simultaneously conducted in our venturi facilities.[6,7] Table 1 summarizes the material-fluid-temperature combinations tested in both facilities.

Only the data obtained in lithium[4] has not been previously published in the open literature. Hence, it is included in Table 2, both for 500°F and 1500°F, since no previous data on cavitation damage in lithium exists to our knowledge even though it is the primary reactor coolant in the SNAP-50 powerplant.

B. Procedure for Lithium. Seven materials were tested in lithium at 500°F (Table 1), but only four of these (T-111, Cb-1Zr(A), and 304 and 316 stainless steels) at 1500°F. Weights were determined before and at various intervals throughout the tests (for the lithium as well as other test fluids) to an accuracy of 0.01 mg. The test fluid was maintained at the required temperature during the test (500°F or 1500°F for lithium) within $\pm$ 5°F. Since the piezoelectric crystals must be maintained below 150°F, the vessel top plate is water-cooled, and a fan provides additional cooling of the crystals.

TABLE 1

SPECIMEN MATERIAL-FLUID-TEMPERATURE
COMBINATIONS INVESTIGATED

Material	Fluid: Water 70°F	Mercury 70°F	Mercury 500°F	Pb-Bi & Li 500°F & 1500°F
1100-0 Al (U-M)	X	...	...	...
2024-T351 Al (U-M)	X	...	...	...
6061-T651 Al (U-M)	X	...	...	...
304 Stainless Steel (U-M)	X	X	Y	Y
316 Stainless Steel (U-M)	X	X	Y	Y
Hot-Rolled Carbon Steel (U-M)	X	X	Y	...
T-111 (Ta-8W-2Hf) (P & W)	X	X	Y	Y
T-222 (Ta-9.5W-2.5Hf-.05C) (P & W)	X	X	...	...
T-222(A) (P & W)	...	...	Y	Y
Mo-1/2Ti (P & W)	X	X	Y	Y
Cb-1Zr (P & W)	X	X	Y	Y
Cb-1Zr(A) (P & W)	X	X	Y	Y
Plexiglas (U-M)	X	X	...	...
Cu(60% cold-worked) (U-M)	X	...	...	...
Cu(900°F anneal, 1 hour) (U-M)	X	...	...	...
Cu(1500°F anneal, 1 hour) (U-M)	X	...	...	...
Cu-Zn(60% cold-worked) (U-M)	X	...	...	...
Cu-Zn(850°F anneal, 1 hour) (U-M)	X	...	...	...
Cu-Zn(1400°F anneal, 1 hour) (U-M)	X	...	...	...
Cu-Ni(60% cold-worked) (U-M)	X	...	...	...
Cu-Ni(1300°F anneal, 1 hour) (U-M)	X	...	...	...
Cu-Ni(1800°F anneal, 1 hour) (U-M)	X	...	...	...
Ni(75% cold-worked) (U-M)	X	...	...	...
Ni(1100°F anneal, 1 hour) (U-M)	X	...	...	...
Ni(1600°F anneal, 1 hour) (U-M)	X	...	...	...

Notes:

1) "X" indicates test conducted for this specimen material-fluid-temperature combination in both the ultrasonic and venturi facilities. "Y" indicates test conducted for this specimen material-fluid-temperature combination only in the ultrasonic facility.
2) The notations (U-M) and (P & W) following the specimen materials indicate the source of the material, namely, The University of Michigan and Pratt & Whitney Aircraft (CANEL), respectively; whereas the notation (A) denotes an annealed condition of the material.

TABLE 2

SUMMARY AND COMPARISON OF CAVITATION RESULTS IN LITHIUM AT 500°F AND 1500°F

	500°F			1500°F		
Material	Avg. Wt. Loss Rate	Avg. MDP Rate	Rating	Avg. Wt. Loss Rate	Avg. MDP Rate	Rating
T-111	1.70 mg./hr.	0.03 mils/hr.	1	0.26 mg./hr.	0.004 mils/hr.	1
T-222(A)	2.48	0.04	2	--	--	-
Mo-1/2Ti	4.61	0.12	3	--	--	-
Cb-1Zr	5.02	0.15	4	--	--	-
304 SS	10.42	0.34	5	1.04	0.034	4
316 SS	10.91	0.36	6	0.81	0.027	3
Cb-1Zr(A)	33.70	1.00	7	0.58	0.017	2

The submergence of the test specimen tip is 1 inch for all tests and the double amplitude 2 mils, as determined by a precision accelerometer[8] attached to the top of the horn and previously calibrated by visual observation of the horn tip with a microscope.

Tests in all the fluids were conducted at the same static suppression pressure. While it would have been preferable to maintain constant suppression head for a more proper modeling of the flow, this was precluded for the heavy liquid metals by vessel pressure-temperature limitations. Since a positive argon gauge pressure was desired at all times to prevent possible in-leakage of oxygen, a value of 15.3 psia was selected for the suppression pressure and maintained constant in all tests. As a result the argon pressure for the 500°F lithium tests was 1.1 psig, since the vapor pressure at this temperature is essentially nil. However, the vapor pressure at 1500°F is about 0.1 psia, so that an argon pressure of 1.2 psig was used for these tests.

A total test duration in lithium of 10 hours was used in all cases except for Cb-1Zr(A) at 500°F which showed very considerable damage after 6 hours, and T-111 at 1500°F which required an exposure of 30 hours to obtain the desired range of total damage.

The lithium was obtained as individual 1/2 pound ingots, hermetically sealed in individual cans, and sized to fit into the cavitation vessel and fill it, upon melting, to the desired level. The ingot was first placed, under argon atmosphere in a dry box at room temperature (for minimum oxygen contamination), into a clean stainless steel beaker sized to fit snugly into the cavitation vessel. Thus, easy removal and

disposal of ingot and beaker at the conclusion of each cavitation test was assured. The sealed cavitation vessel was then removed from the glove box, placed in the furnace, and heated to the desired temperature. Each test used a fresh ingot and beaker. This procedure results in a very economical facility design, and keeps oxide contamination relatively uniform and at a minimum.

After each run the vessel was removed from the furnace and cooled to a temperature ($\sim$375°F) slightly in excess of the lithium melting point but below the ignition temperature. The vessel was then opened and the horn-specimen assembly removed, after which the vessel was further cooled and the beaker with the lithium removed and discarded. Excess lithium adhering to the test specimen and horn was easily removed by dipping the assembly into cold water. The lithium-water reaction under these circumstances was not particularly vigorous. Further details of the test procedures are reported elsewhere.[4]

C. Results in Lithium. The lithium damage data in terms of mean depth of penetration* versus test duration is plotted in Figures 4 and 5 and listed in Table 2. As will be noted from these curves, the tantalum-base alloys [T-111 and T-222(A)] are by far the most damage resistant at either temperature. The position of the Cb-1Zr(A) improves relative to the stainless steels at the higher temperature, as would be expected, since its mechanical properties are less temperature-dependent.

---

*Volume removed (as inferred from weight loss) divided by exposed area.

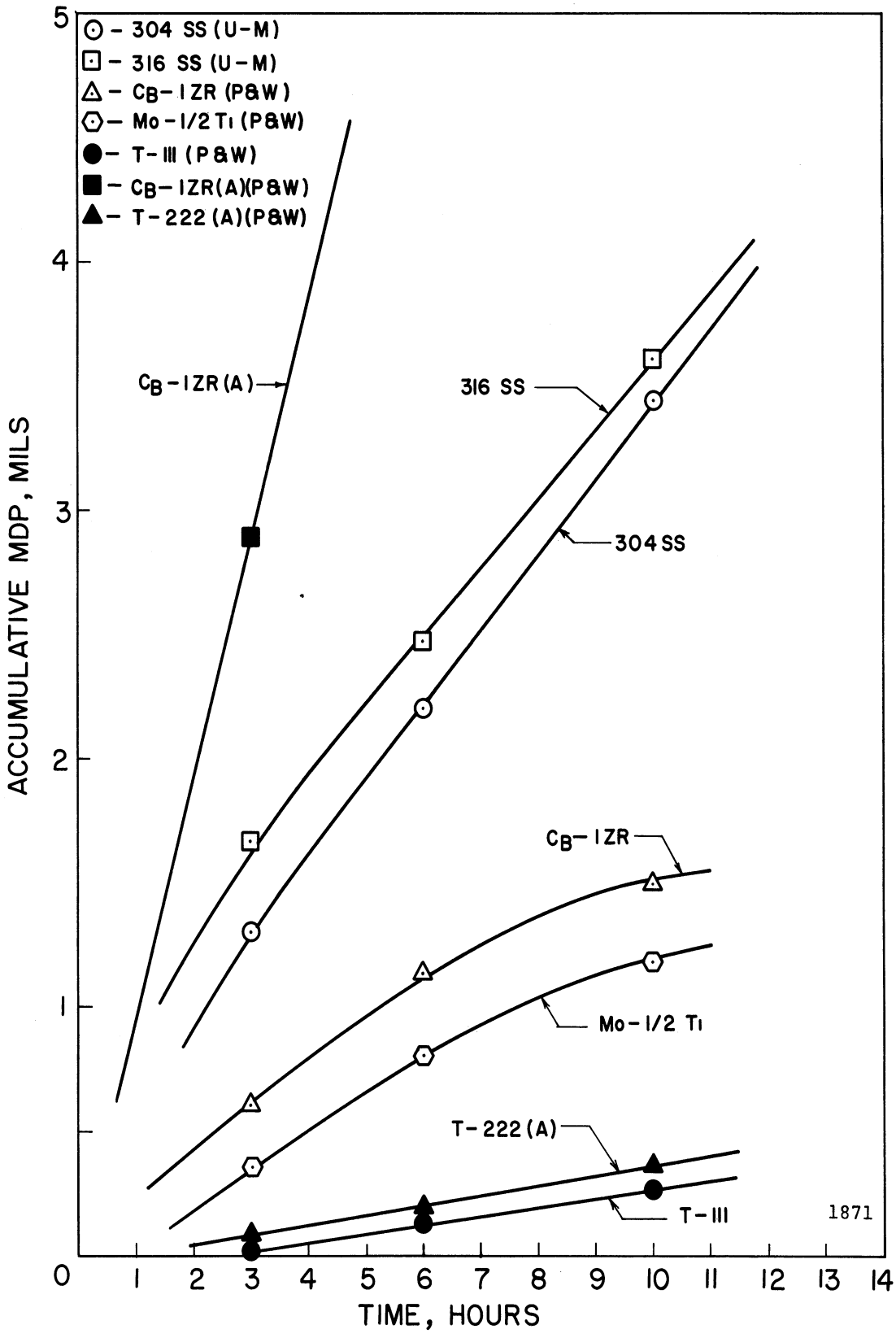

Fig. 4.--Effect of cavitation test duration on MDP at 500°F in lithium.

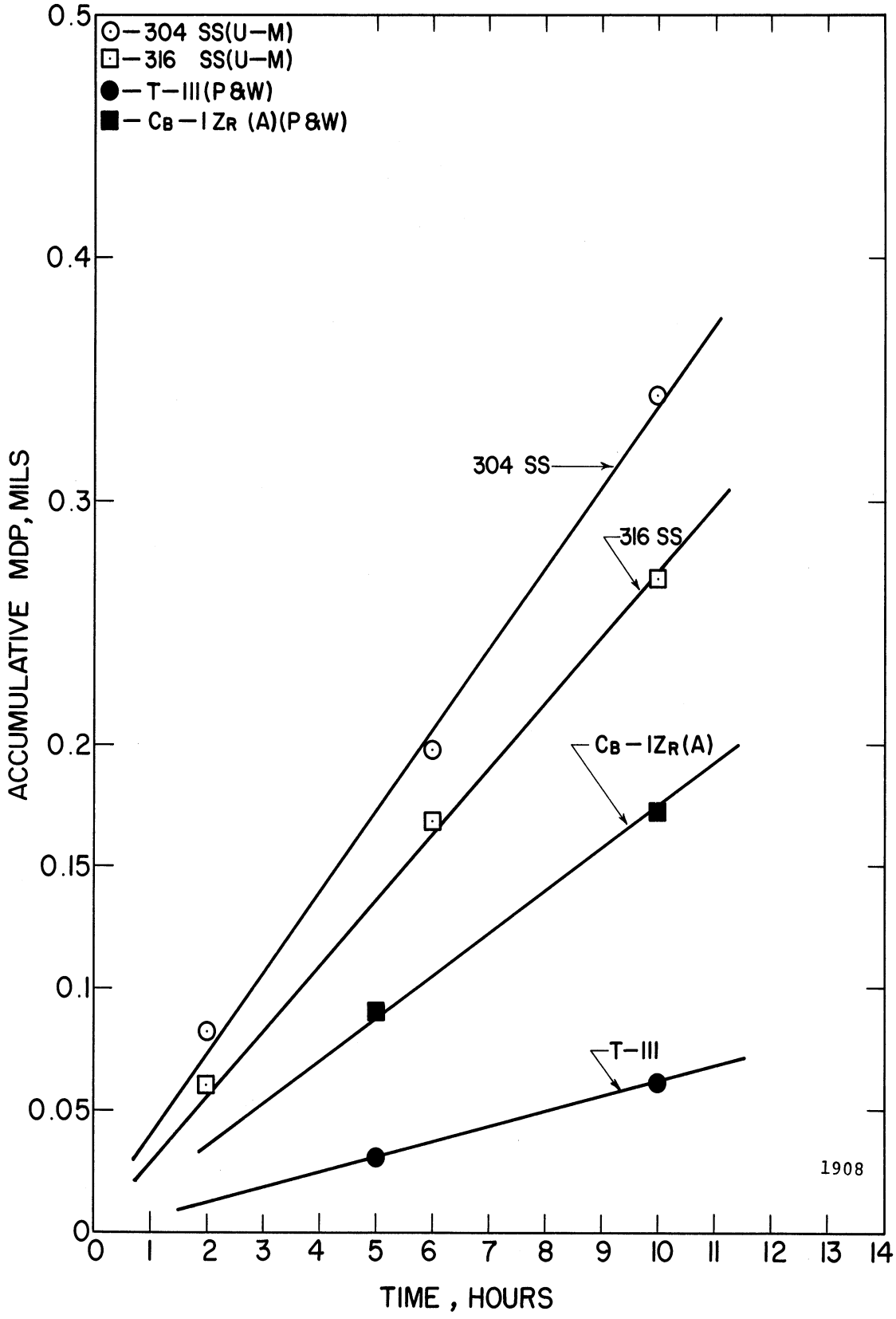

Fig. 5.--Effect of cavitation test duration on MDP at 1500°F in lithium.

The materials are rated in Table 2, based on ability to resist cavitation erosion.

Note especially that the damage has decreased by an order of magnitude for any of the materials when the temperature was increased from 500°F to 1500°F. As will be discussed later, the precisely opposite effect had been observed in tests with lead-bismuth alloy over the same temperature range.[2,4]

For comparison with other tests, the average mean depth of penetration rate (MDPR) is computed for each test, neglecting the very early part. It is approximately constant during the test for most materials. In our experience, as already discussed in greater detail elsewhere,[3] an approximately constant rate will continue, after the very early relatively unpredictable portion of the test, as long as the damage remains fairly uniformly distributed across the surface. This condition of uniform damage persisted to a much larger total MDP for the heavy liquid metal tests[2,3,4] than for either the water[4] or the present lithium tests, and hence the uniform damage rate also persisted, in some cases, to total MDP as large as 50 mils.[3,4]

Figures 6 and 7 show the condition of the test specimens at the conclusion of the test at 500°F and 1500°F, respectively. Type 316 stainless steel specimens from the lead-bismuth, mercury, and water tests are shown in Figure 8 for comparison. The damage to the mercury and lead-bismuth specimens is uniformly distributed over the surface (there is, however, a very small undamaged ring around the outside), even though the total volume removed is much greater than that in the

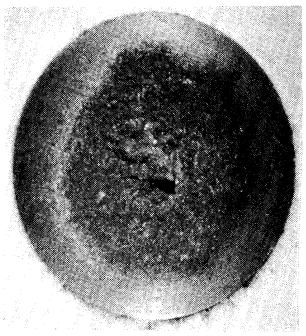

(1) T-111(P & W)
10 Hour Exposure

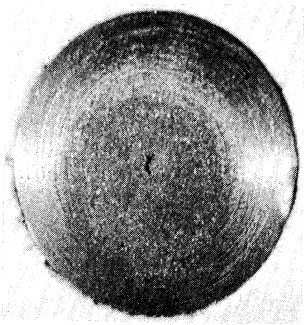

(2) T-222(A)(P & W)
10 Hour Exposure

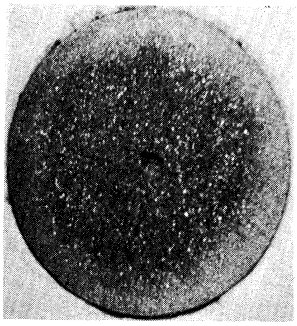

(3) Mo-1/2Ti(P & W)
10 Hour Exposure

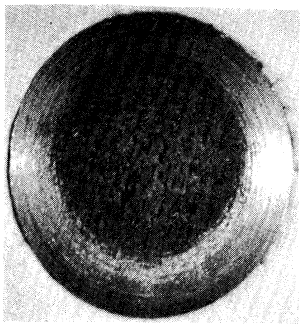

(4) Cb-1Zr(P & W)
10 Hour Exposure

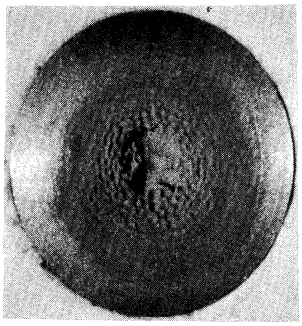

(5) 304 SS(U-M)
10 Hour Exposure

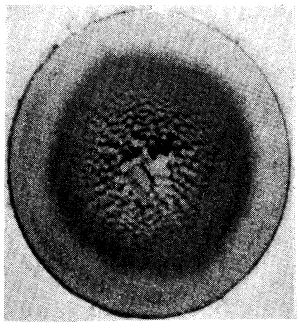

(6) 316 SS(U-M)
10 Hour Exposure

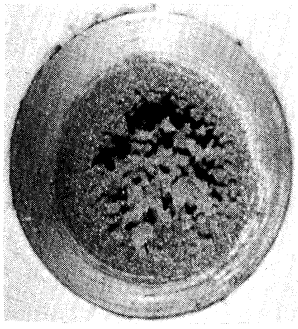

(7) Cb-1Zr(A)(P & W)
6 Hour Exposure

1906

Fig. 6.--Photographs of specimens subjected to cavitation damage in lithium at 500°F.

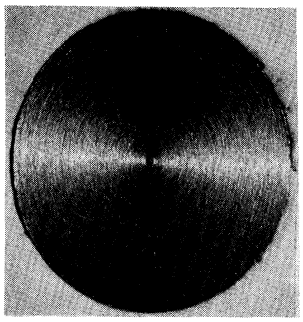

(1) T-111(P & W)
10 Hour Exposure

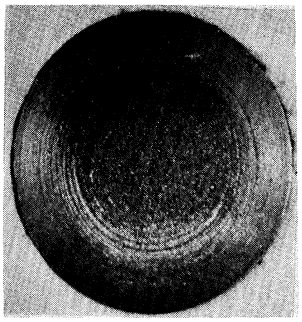

(2) Cb-1Zr(A)(P & W)
10 Hour Exposure

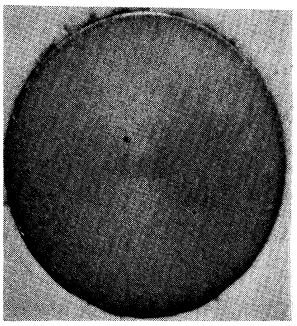

(3) 316 SS(U-M)
10 Hour Exposure

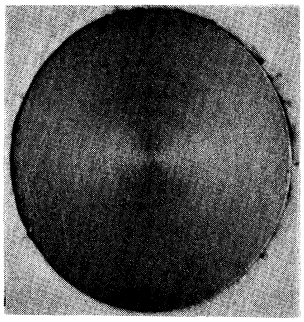

(4) 304 SS(U-M)
10 Hour Exposure

1909

Fig. 7.--Photographs of specimens subjected to cavitation damage in lithium at 1500°F.

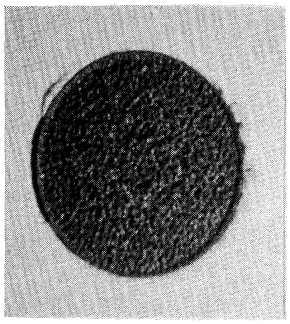

(1) 12 Hour Exposure
Pb-Bi at 500°F

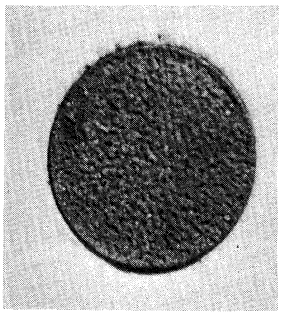

(2) 6 Hour Exposure
Pb-Bi at 1500°F

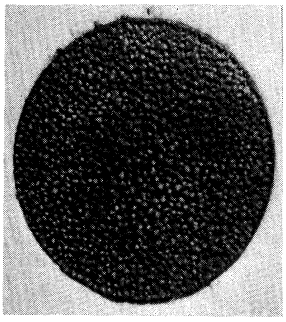

(3) 12 Hour Exposure
Mercury at 500°F

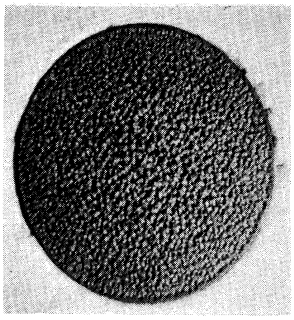

(4) 12 Hour Exposure
Mercury at 70°F

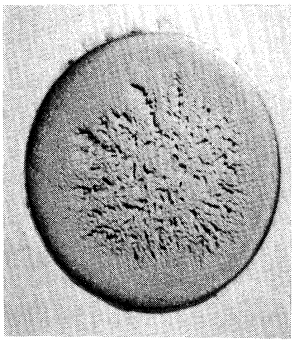

(5) 36 Hour Exposure
Water at 70°F

2351

Fig. 8.--Photographs of type 316 stainless steel specimens subjected to cavitation damage in lead-bismuth, mercury, and water.

water and lithium tests. However, in the water tests and even more so in the lithium tests, the damage is concentrated toward the center with large undamaged areas around the outside. This difference in damage pattern is believed due to the already mentioned large differences in suppression head (NPSH) between the fluids, so that the flow regimes are not properly modeled. The suppression of cavitation and damage around the outer edge is believed due to the formation of a ring-vortex adjacent to that location, leading to an increase in pressure on the specimen surface near the edge.[9,10] This small pressure increase becomes important in suppressing cavitation as the NPSH is raised, i.e., for the lower density fluids.

D. Corrosion Effects. Examination of the horn, beaker, and sides of the test specimens, all of which were not cavitated, but were submerged in the test fluid (in the case of the horn for the total duration of many tests), indicated that corrosion effects in the absence of cavitation were negligible, as would be expected for these relatively short durations.[11] This was true for all the fluids tested.

Figure 9 is a 100X photomicrographic section through the surface of a 304 stainless steel specimen cavitated in lithium at 500°F for 10 hours, while Figure 10 is a 500X section from the same specimen taken just below the surface. There is no evidence of corrosion on the surface (corrosion products may have been removed by the scouring action of the cavitation). Also, there is no evidence of intergranular corrosion below the surface. Cross-section examination of specimens from the lead-bismuth tests at 1500°F similarly provided no evidence of corrosion.

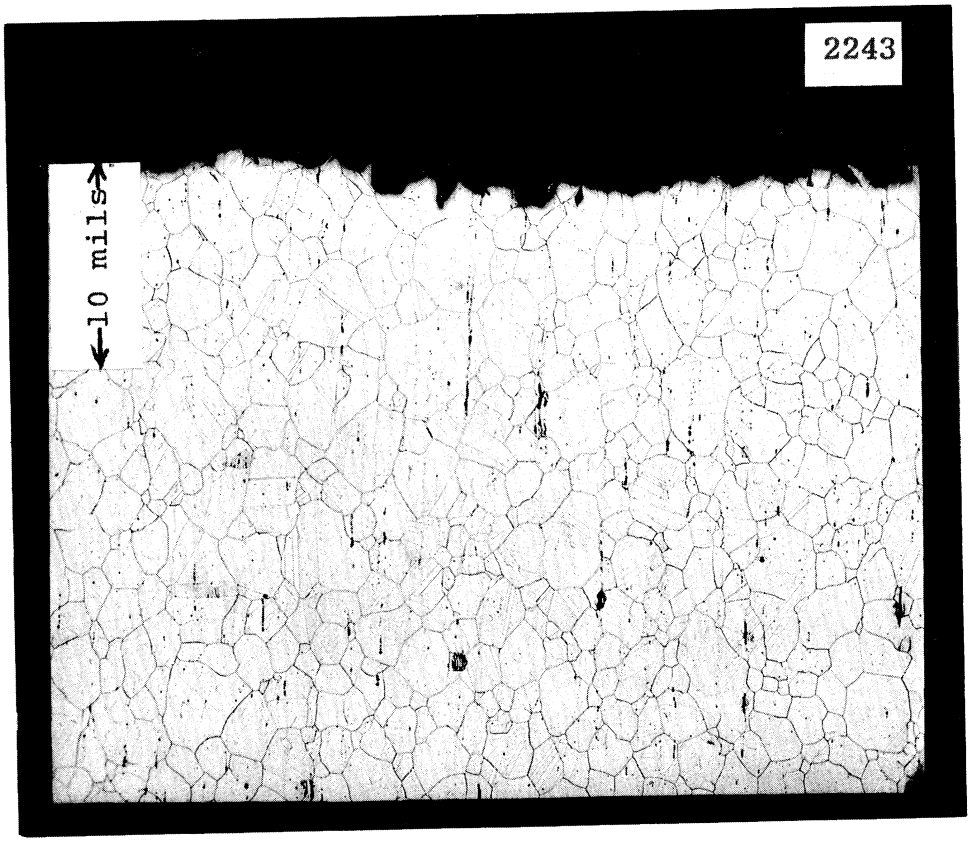

Fig. 9.--Photomicrograph of type 304 stainless steel specimen tested in lithium at 500°F (specimen surface, magnification 100X).

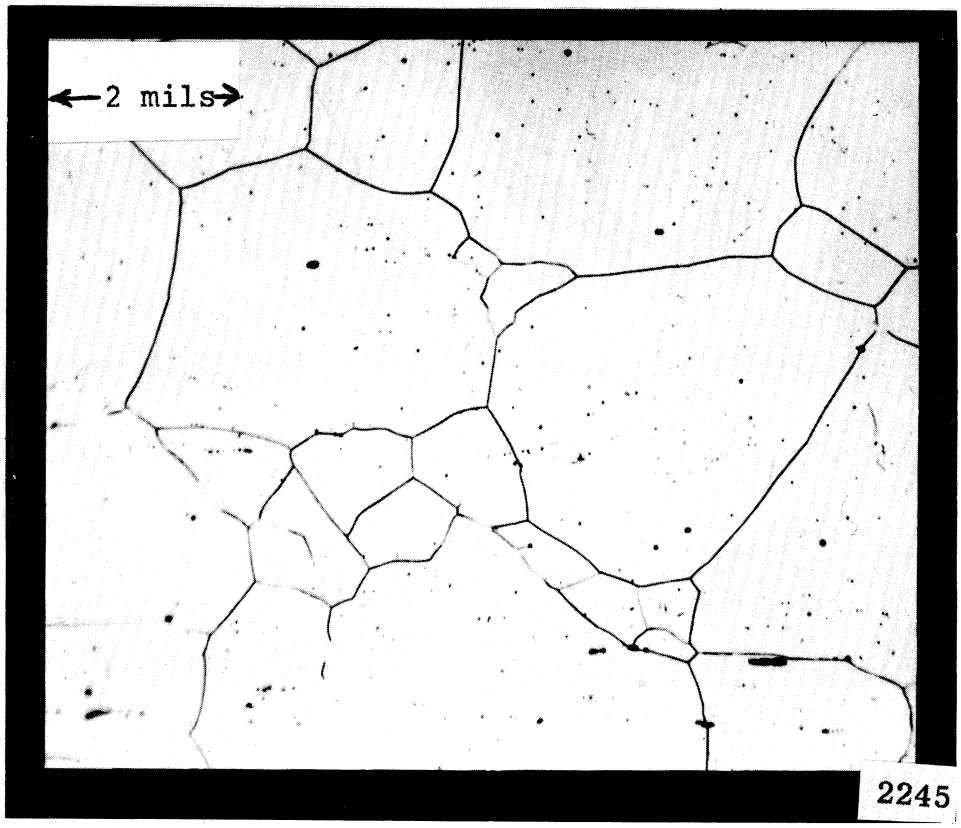

Fig. 10.--Photomicrograph of type 304 stainless steel specimen tested in lithium at 500°F (interior of specimen, magnification 500X).

Specimens examined included 316 stainless steel, T-222(A), and Cb-1Zr(A).[4] While it cannot be concluded that chemical effects are of negligible importance in these tests, there is also no evidence to support their importance. Pulsed-type tests similar to those used by Plesset in water[12] would be necessary to further clarify this issue.

IV. THERMODYNAMIC EFFECTS

A. General. As perhaps first suggested about 10 years ago,[13] it has come to be accepted that fluids showing strong "thermodynamic" effects do not cavitate as readily or to the extent of "conventional" fluids (cold water, e.g.), nor is cavitation as damaging in such fluids. Very qualitatively, the measure of this tendency is the thermodynamic parameter, B, which is the ratio of vapor volume formed to liquid volume supplying the necessary heat of vaporization when the suppression head (NPSH) is reduced by unity[14] adiabatically under conditions of thermal equilibrium. That damage with such fluids is reduced is presumably a result of the "cushioning" of collapse by trapped vapor which cannot condense sufficiently rapidly, and, hence, behaves as a non-condensible gas during the final portion of the bubble collapse process.

It has long been known that this effect is also operative in vibratory cavitation damage tests.[15,16,17,18] If such tests are conducted at atmospheric pressure in water, it is found that the damage rate peaks sharply at about 50°C, falling off to near zero both at lower and higher temperatures. Figure 11 shows the result of such a test[19] recently conducted here. It is clear that the damage would decrease

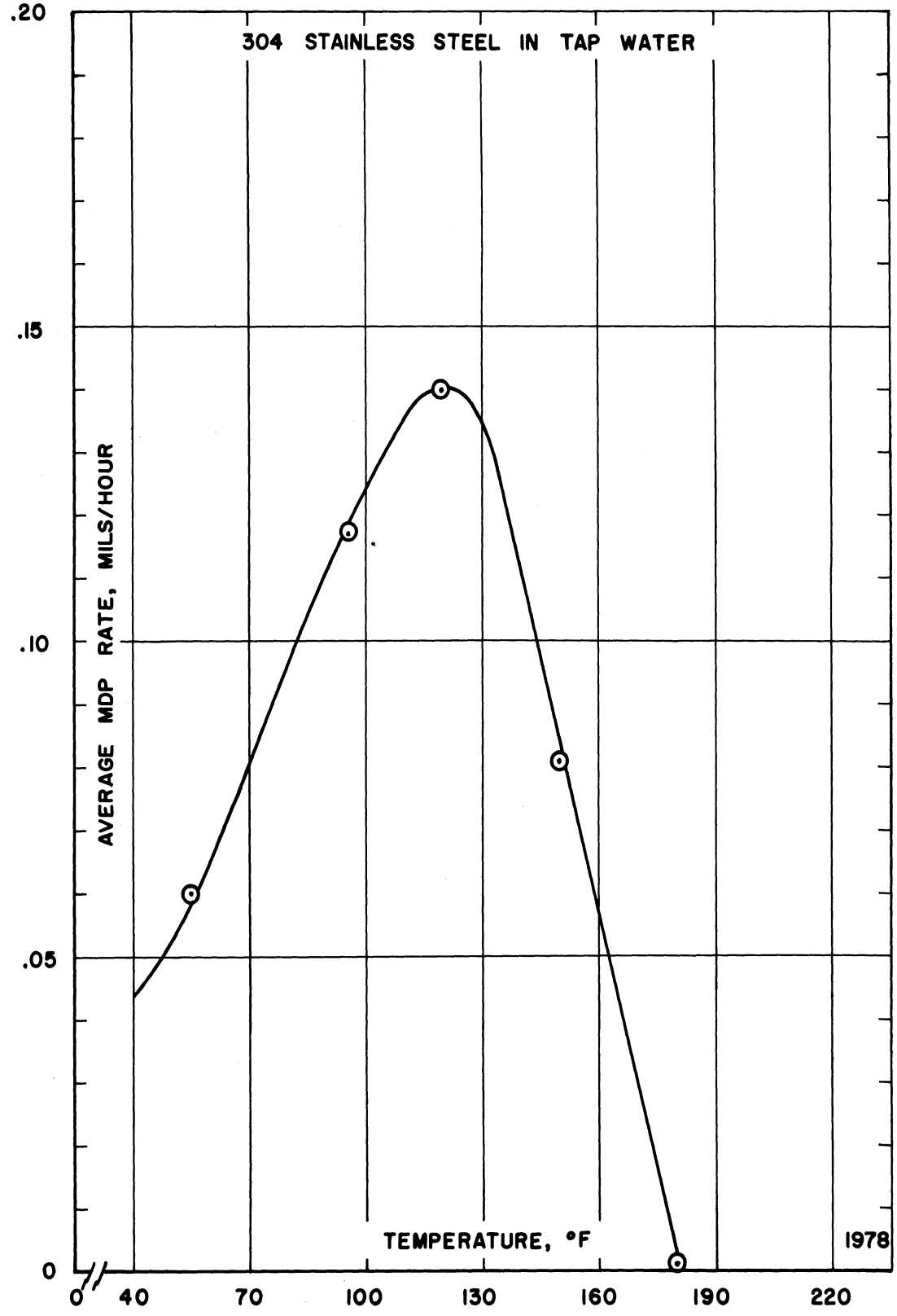

Fig. 11.--Effect of temperature on cavitation damage in water--type 304 stainless steel specimen.

somewhat at high temperature due to reduction of static NPSH. However, it seems logical that the very large decrease in damage at temperatures where NPSH is still appreciable is primarily due to vapor cushioning involved with the "thermodynamic effect."

The damage decrease at lower temperature in water has been assumed due to cushioning from increased non-condensible gas in the water due to increased solubility at low temperature.[17] However, this effect would not apply to tests with molten metals where the gas solubility is essentially nil at any temperature. The decrease in damage at lower temperature in water may also be partially due to increased viscosity and decreased chemical activity, mechanisms which might apply to liquid metals. A single test of type 304 stainless steel in lithium at 400°F did indicate a small reduction in damage rate from the 500°F tests.

The presently available liquid metal vibratory cavitation damage data, where examination of this effect is possible, includes our own tests and also tests in sodium at both 500°F and 1500°F conducted by Hydronautics, Inc.[20,21] From these various tests it appears that the thermodynamic effect was important for lithium and sodium at 1500°F (but not at 500°F), water at room temperature, but <u>not</u> mercury at room temperature or 500°F, nor lead-bismuth alloy at 500°F or 1500°F. Since the vapor pressure of lithium at 1500°F (where there was an effect) is an order of magnitude less than that of mercury at 500°F (where there was no effect), it is clear that the reduction of damage sometimes encountered at high temperature is not to be explained unaided on the

basis of vapor pressure or NPSH alone, as some of the previous investigators have tentatively suggested.[15,17,22]

B. Detailed Consideration. The vapor-cushioning mechanism previously mentioned can only exist when there is an appreciable quantity of vapor in the collapsing bubbles, and when the latent heat from this vapor as it condenses cannot be conducted away into the liquid at sufficient rate to prevent a substantial local rise in temperature, which would then terminate the condensation process until the vapor pressure had attained the new saturation level. With small enough heat conduction rates in the liquid it is clear that the vapor would behave essentially as a non-condensible gas, and thus terminate the collapse. Since the thermodynamic parameter, B, already discussed, does not involve heat transfer rates, it is clearly inadequate for the present purpose.

This overall problem is of general importance in two-phase flow phenomena and, hence, has been examined by several investigators.[23,24,25,e.g.] Of these, the recent study by Florschuetz and Chao[23] seems best adapted to the present purpose in its relatively rigorous consideration of the pertinent mechanisms. In this paper a revised thermodynamic parameter, $B_{eff.}$, is defined:

$$B_{eff.} = \left(\frac{\rho_L C_L \Delta T}{\rho_v L} \right)^2 \frac{K_L}{R_0} \left(\frac{\rho_L}{\Delta p} \right)^{1/2} \quad (1)$$

where:

ρ_L = liquid density, lbm./ft.^{3}

ρ_v = vapor density, lbm./ft.^{3}

C_L = specific heat of the liquid, Btu/lbm.°F

ΔT = temperature drop in liquid film due to vaporization, °F

L = latent heat of vaporization, Btu/lbm.

K_L = thermal diffusivity of the liquid, ft.^{2}/hr., = $k_L / \rho_L C_L$

k_L = thermal conductivity of the liquid, Btu/hr.ft.°F

R_0 = equilibrium bubble radius, ft.

Δp = decrease in liquid pressure corresponding to a decrease ΔT in liquid temperature, lbf./ft.^{2}

$B_{eff.}$ can be expressed in terms of B, as:

$$B_{eff.} = B^2 \frac{K_L}{R_0} (NPSH)^{3/2} \qquad (2)$$

They show that for low $B_{eff.}$ bubble growth and collapse are heat transfer controlled, i.e., "thermodynamic" effects are important, and for high $B_{eff.}$ (fluids such as cold water), these processes are inertia controlled.

To compute $B_{eff.}$ it is necessary to assume values for R_0 and NPSH. For the present purpose, we have assumed nominal values of 1 cm. for the former and 1 ft. for the latter. Hence, the present numerical results reflect these assumptions. The justification for the use of constants for these two parameters follows. The NPSH seen by the growing and collapsing bubbles in a vibratory facility is composed both of a steady-state (static) and a transient component, the latter being induced by, and in phase with, the motion of the horn. Since the transient component is relatively large compared to the static, it may be reasonable to assume that the "effective" NPSH is constant. This

directly justifies a constant value for NPSH in calculating $B_{eff.}$. If so, R_0 would also be constant to a first approximation.

The values of the applicable thermodynamic parameters (B and $B_{eff.}$) for the fluids and temperatures of interest are listed in Table 3. Examination of equation (1) indicates that the following factors among others lead to important thermodynamic effects: large latent heat of vaporization (condensation) and vapor density; small thermal diffusivity, specific heat, and density of the liquid. Vapor pressure enters only as it affects vapor density. Thus, the potential importance of thermodynamic effects cannot be delineated simply by vapor pressure. The ordering of $B_{eff.}$ (Table 3) according to the various fluid-temperature combinations is hopeful in that from the cavitation damage data it is clear that the thermodynamic effect is operative for the higher temperature water tests, and the 1500°F sodium and lithium tests, but not for the mercury or lead-bismuth tests at either test temperature.

C. Application to Present Data. The thermodynamic parameter, $B_{eff.}$, can be applied quantitatively to the present data only if that data can be normalized in a fashion to remove its dependence upon other effects and mechanisms. This has been accomplished by using the data for type 304 stainless steel (Table 3). A thermodynamic effect correction to cavitation damage data derived for this material should, at least approximately, be applicable to any material.

To remove the effect of fluid property dependence other than through the thermodynamic effect, the data for each fluid has been normalized to a given data point in that fluid. These results are listed in Table 3.

TABLE 3

VALUES OF THERMODYNAMIC PARAMETER AND CORRECTED NORMALIZED MDP RATE FOR VARIOUS FLUID-TEMPERATURE COMBINATIONS

Fluid and Temperature	B	$B_{eff.}$	MDP Rate	Norm. MDP Rate	Material Temperature Correction	Corrected Normalized MDP Rate
Water - 55°F	4.69×10^3	174.0	0.06 mils/hr.	0.43	1.0	0.43
Water - 95°F	413.0	1.35	0.11	0.79	1.0	0.79
Water - 120°F	111.1	0.10	0.14	1.0	1.0	1.0
Water - 150°F	27.4	0.006	0.08	0.57	1.0	0.57
Water - 180°F	7.7	0.0005	0.001	0.007	1.0	0.007
Mercury - 70°F	3.28×10^{12}	2.72×10^{21}	0.32	1.0	1.0	1.0
Mercury - 500°F	1.14×10^3	644.0	0.69	2.2	0.81	1.78
Lithium - 500°F	4.41×10^{14}	2.02×10^{26}	0.34	1.0	1.0	1.0
Lithium - 1500°F	206.0	48.9	0.034	0.1	0.129	0.0129
Lead-Bismuth--500°F	5.04×10^{24}	1.73×10^{46}	0.93	1.0	1.0	1.0
Lead-Bismuth--1500°F	3.30×10^9	8.49×10^{15}	11.30	12.2	0.129	1.57
Sodium - 500°F	5.42×10^8	1.12×10^{15}	0.53*	1.0	1.0	1.0
Sodium - 1500°F	2.04	0.01	0.00033*	0.0006	0.126	0.000076

*Type 316 stainless steel tested by Hydronautics, Inc. (References 20 and 21).

It is next necessary to remove the dependence upon material properties, as they are affected by the different test temperatures, as far as possible. For this purpose an approximate material property damage-predicting equation, derived from the data as a whole and to be discussed later, was used, i.e., as an example, the 1500°F lithium damage data is to be multiplied by a factor less than unity (actually 0.129 from Table 3) to make it directly comparable to the 500°F lithium data, since the test material is severely weakened at 1500°F as compared with 500°F. When this correction had been applied, the "Corrected Normalized MDP Rate" results. Note that the correction factor for the water data is unity since the temperature variation for this set is not sufficient to affect the properties of the test material. The "Corrected Normalized MDP Rate" should now be unity for those cases where the thermodynamic effect is not operative, and less than unity for those cases where either this effect or other effects such as increased gas content for water, e.g., may act to reduce the damage. However, in the cases of mercury at 500°F and lead-bismuth at 1500°F, values somewhat greater than unity were obtained. This cannot be due to the thermodynamic effect since increased vapor content, etc., can only act to reduce damage as the mechanism is presently understood. The increase in damage for these high temperature tests, over and above that forecast by the predicting equation based on mechanical properties, can be due either to the inaccuracy of the predicting equation or to increased chemical activity at the higher temperature, lower viscosity, changes in surface tension, etc. The test data scatter itself is not of sufficient order

to explain these discrepancies. For the purpose of examining the thermodynamic effect, those values greater than unity were assumed unity.

In Figure 12, the Log Corrected Normalized MDP Rate (Table 3) is plotted against Log $B_{eff.}$ (Table 3) for the liquid metals. Figure 13 is a similar plot for the water data, which was plotted separately since it involves the complicating factor of dissolved gas effects. For those fluid-temperature conditions for which the logarithm of the corrected rate is zero, the thermodynamic effect is negligible, while the correction factor to be applied for this effect to fluid-temperature conditions to the left of the break in the curve is indicated. Tests in mercury at somewhat higher temperature to determine more accurately the break in the curve would be desirable. A dashed vertical line through this break-point has been used to indicate an approximate division between regions of heat transfer and inertia control and corresponds to a value of $B_{eff.} = 1000$.

The comparable curve for the water data (Figure 13) includes a dotted curve to illustrate the position and shape of a curve influenced only by the thermodynamic effect (effect of dissolved gas is negligible), assuming again that a value of $B_{eff.} = 1000$ is the division between inertia control and heat transfer control. The actual data points (Table 3) determine the solid curve which is to be used for the correction factor for water.

Figure 14 shows Log $B_{eff.}$ as a function of fluid temperature for the various fluids considered.

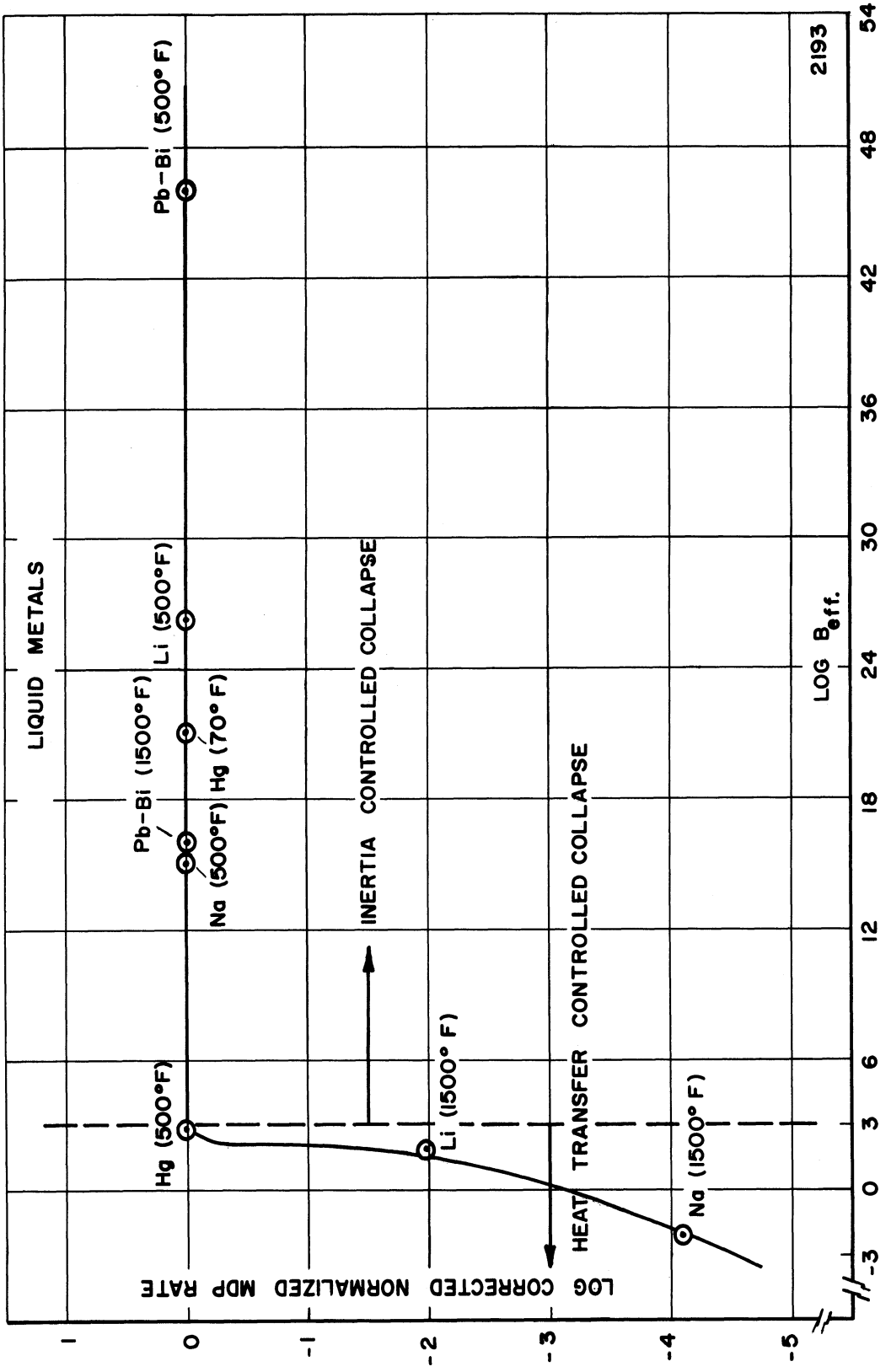

Fig. 12.--Effect of thermodynamic parameter on cavitation damage--liquid metals.

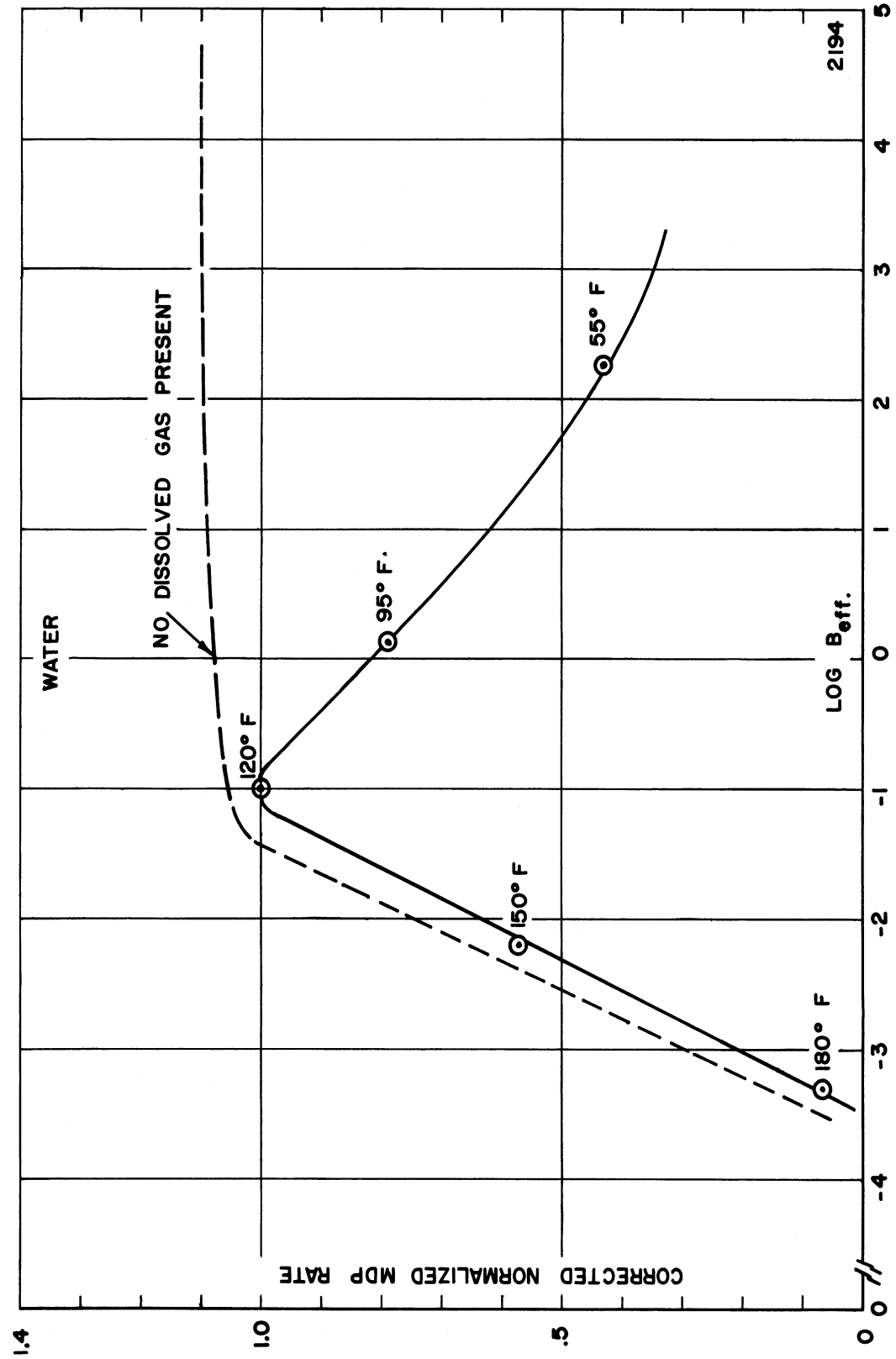

Fig. 13.--Effect of thermodynamic parameter on cavitation damage--water.

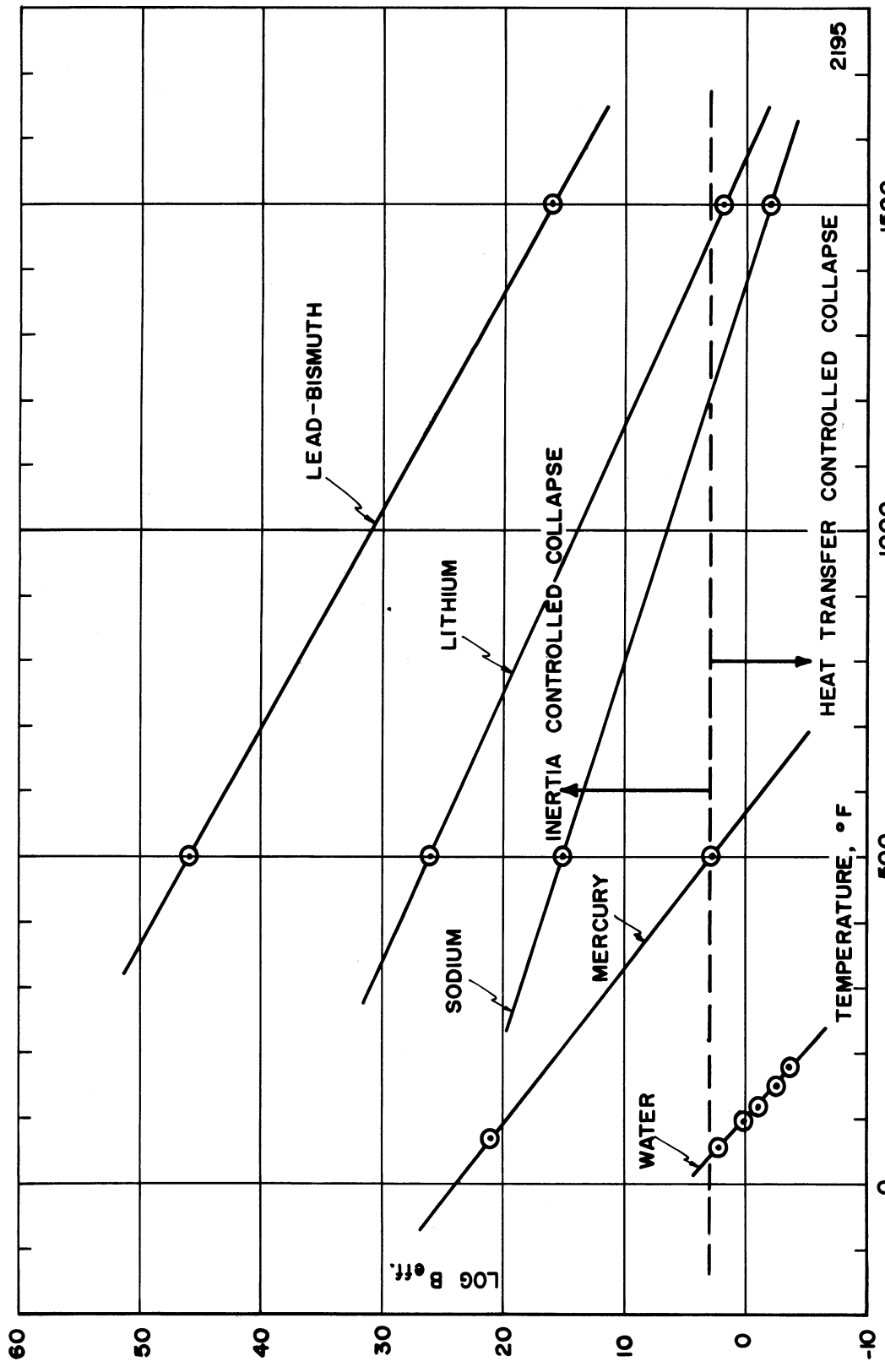

Fig. 14.--Effect of temperature on the thermodynamic parameter--liquid metals and water.

Figures 12, 13, and 14 can be used to approximate the change in damage to be anticipated in a given fluid for a change in operating temperature, if NPSH and degree of cavitation are constant, and if a separate correction is made for the change in material properties accompanying a temperature change.

V. CORRELATION OF CAVITATION DAMAGE WITH MECHANICAL AND FLUID PROPERTIES

A. General. Attempts to correlate cavitation damage data both from the venturis[6,7] and from the vibratory facility[2,3,4] individually have already been reported. A least mean square fit regression analysis was used wherein it was attempted to represent the MDPR in terms of a power series involving various applicable material and fluid properties, each term multiplied by a suitable coefficient and raised to selected exponents. This computer program has been described previously in detail.[2,4,26,27]

In general, it was found that arbitrarily good correlations could be obtained if a sufficient number of terms were allowed, but no relatively simple, reasonably precise, correlation applicable to more than small subsets of the data could be found in terms of the relatively standard fluid and material mechanical properties. These latter included tensile strength, yield strength, engineering strain energy, true strain energy, hardness, elongation, reduction in area, and elastic modulus (each property having been defined earlier for the present purposes).[3,6,28]

Very recently Hobbs[18] reported that he obtained the best correlation with "ultimate resilience" for his vibratory data for a variety of materials in water. We have found very recently that this parameter also provides the best correlating parameter for our own data. As here used, ultimate resilience is the energy per unit volume required to stress the material to the true breaking stress, assuming no plastic deformation (Figure 15). To justify the use of this parameter it must be assumed that the loading rate in cavitation attack is so great that "brittle fracture" is the common mode of failure. It is true that examination of test specimens often does support this viewpoint. It is also true that very strong materials with low ductility, such as stellites, tool steels, etc., show very great cavitation damage resistance as compared with ductile materials of lower strength but comparable strain energy to failure (engineering strain energy). Hence, very qualitatively, ultimate resilience appears to be a potentially successful correlating parameter.

B. Initial Application to Present Data. To obtain a correlation between cavitation damage and material properties using our presently available data, it is clear that that portion of the data obviously influenced by "thermodynamic effects" should not be considered. Even when this is omitted, it is still necessary to take some account of fluid properties if data obtained in different fluids is to be used. The most prominent fluid property variation in the present data is that of density (about 0.5 g./cc. for lithium and 13.6 g./cc. for mercury). Therefore, the total data set, excluding the 1500°F lithium data (since

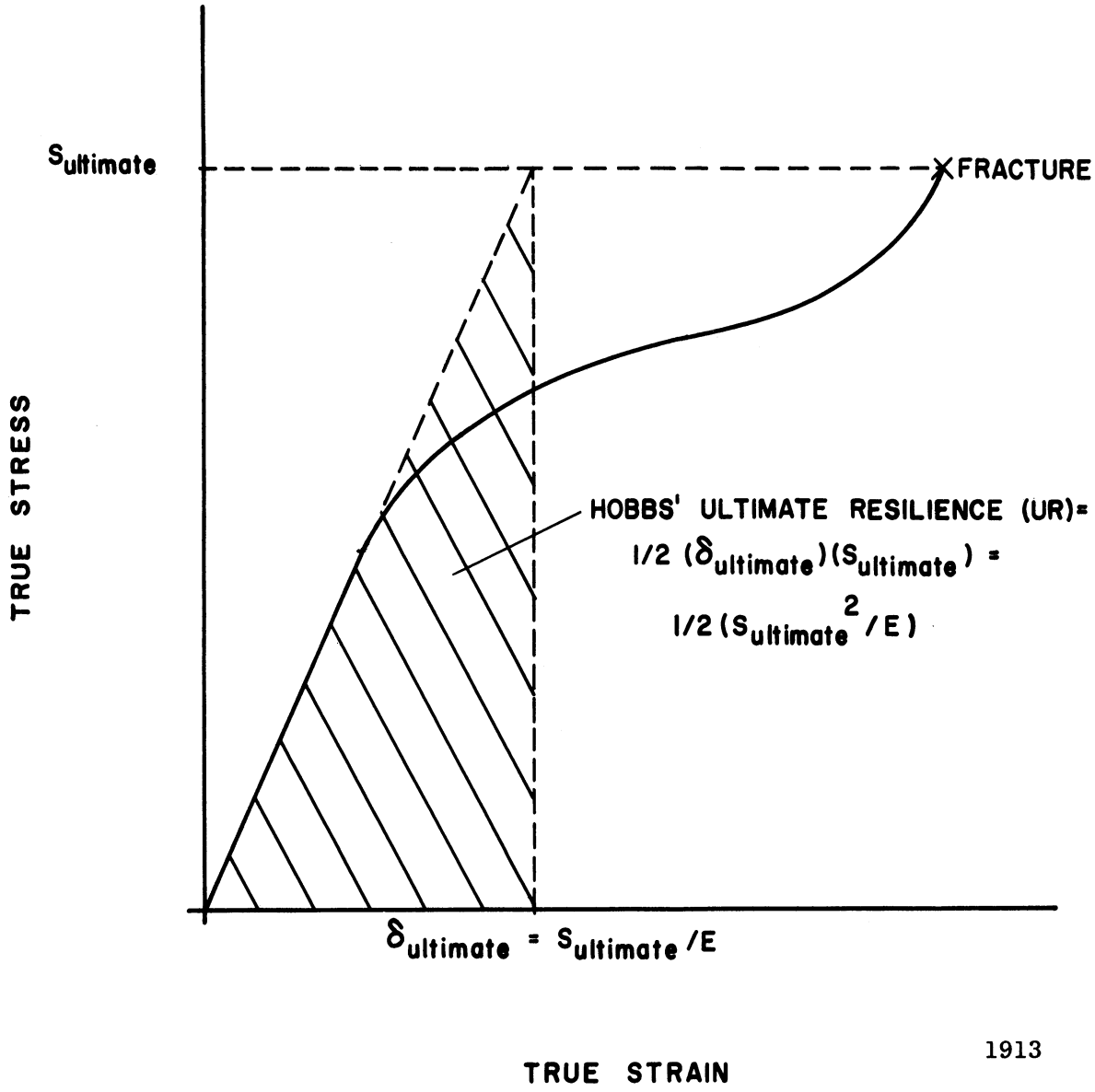

Fig. 15.--True stress-strain curve showing Hobbs' ultimate resilience concept.

it was obviously influenced grossly by thermodynamic effects), was subjected to the correlation program which was allowed to consider all the mechanical properties previously mentioned (including the ultimate resilience) and fluid density. The best correlation obtained included only ultimate resilience of the material properties and also density, a highly encouraging result in view of the highly complex and imprecise results which had been obtained before the inclusion of ultimate resilience among the possible mechanical properties.

C. Final Damage Predicting Equations. To obtain a "final" predicting equation, as generally applicable as possible, it is necessary to include a correction for the thermodynamic effect, and also for the fact that static NPSH varied over a factor of about 30 for these tests. As previously mentioned, the effect of increasing NPSH appeared to be a reduction of damage, as an increasingly large undamaged annulus adjacent to the specimen outside diameter and a concentration of damage toward the center were noted. Thus, the damaged area is decreased as NPSH increases. Very roughly it was estimated that the decrease in damaged area between mercury and water was by a factor of ~ 2. If it is assumed that the total NPSH including the transient component is about the same for all fluids, since it is dominated by the transient component which depends primarily on the specimen accelerations, then the number of bubbles per unit area of bubble cloud may remain fairly constant. Hence, the number of bubbles seen by the specimen surface would also be roughly proportional to the damaged area. Since the ratio of the damaged areas between mercury and water was about 2, the correction

factor to be applied to the water data, taking the mercury as a standard, is precisely 2. The NPSH correction can be expressed as the ratio of NPSH values of mercury (standard) and the fluid in question, raised to a suitable exponent to match the mercury-water comparison already cited. Thus:

$$\left[\frac{(NPSH)_{H_2O}}{(NPSH)_{Hg}}\right]^{n} = 2 = \text{Ratio of damaged areas}$$

$$[(35.3)/(2.60)]^{n} = 2; \quad n = 0.266$$

Then for lithium we have:

$$\left[\frac{(NPSH)_{Li}}{(NPSH)_{Hg}}\right]^{0.266} = [(70.6)/(2.60)]^{0.266} = 2.41$$

In a similar fashion the correction factor to be applied to the lead-bismuth data is found to be 1.075. Thus, the cavitation damage data obtained in water, lithium, and lead-bismuth alloy should be increased by the above appropriate factors to take account of the variation in bubble population due to the variation in static NPSH.

The correction factor to be applied to the data for the thermodynamic effect can be determined directly from Figure 12 for liquid metals and from Figure 13 for water (in which case it also includes the correction for dissolved gas). Note that the correction factor to be applied to the experimental data is the inverse of the corrected normalized MDP rate taken either from Figure 12 or 13. In the present case

this correction for thermodynamic effect is unity except for the 1500°F lithium data and the water data. All the raw experimental data is then multiplied by the two correction factors, one for thermodynamic effect and one for variation in static NPSH. This corrected data was then subjected to the correlating program, which was allowed only ultimate resilience and fluid density as correlating parameters, since, as already discussed, these had been most successful with the limited data set previously used. A choice among the exponents: ± 1, ± 2, $\pm 1/2$, ± 3, and $\pm 1/3$, was allowed by the program. The statistically best predicting equation then generated involved only ultimate resilience, since apparently the previous density dependence was removed through the NPSH correction:

$$MDPR = 0.142 + 8.918(UR)^{-1/2}$$

Coefficient of Determination* = 0.780

Average Algebraic % Deviation** = 51.3%

Average % Deviation*** = 139.0%

---

*The coefficient of determination[26,27] is a statistical quantity that can be interpreted as the proportion of the total variation in the dependent variable that is explained by the predicting equation. Its values range from 0 (no prediction) to 1.0 (perfect prediction). It is here considered as the figure of merit for the correlation obtained.

**The percent deviations between the experimental and predicted values of MDP rate are algebraically summed. The average algebraic percent deviation is then the algebraic sum divided by the number of data points.

***The percent deviations between the experimental and predicted values of MDP rate are summed without regard to algebraic sign. The average percent deviation is then this total deviation divided by the number of data points.

A complete predicting equation would then be of the form:

$$MDPR = C_1 \cdot C_2[0.142 + 8.918(UR)^{-1/2}] \quad (3)$$

where C_1 is the correction for variation in static NPSH and can be computed as:

$$C_1 = 1.29(NPSH)^{-0.266}$$

C_2 is the correction for thermodynamic effect and is exactly the corrected normalized MDP rate plotted in Figures 12 and 13. Note that:

$$0 < C_1 < 1 \quad \text{and} \quad 0 < C_2 < 1$$

While the statistical precision of equation (3) is not as good as might be hoped, it is recommended by its simplicity. The precision is sufficient for engineering estimates, and may be the best that can be expected considering the great complexity of the cavitation phenomenon.

An alternate predicting equation was obtained by treating the data without correcting for varying NPSH. This form includes the density and still retains the inverse square root dependence on ultimate resilience. It is statistically somewhat less suitable than equation (3):

$$MDPR = C_2[0.284 + 7.254(UR)^{-1/2} - 0.331(\rho)^{-2}] \quad (4)$$

Coefficient of Determination = 0.744

Average Algebraic % Deviation = 49.5%

Average % Deviation = 164.7%

It is clear from the above that density and/or NPSH must be somehow considered. Since in the present data NPSH always varies in

proportion to $1/\rho$, there is no way to separate the effect of these two parameters. Hence, further tests where one is varied while the other is maintained constant are necessary.

D. Comparison With Other Correlating Parameters. A final check to determine the relative merit of ultimate resilience as a damage correlating mechanical property was made by obtaining optimum single-property correlations with other mechanical properties which have been previously considered as potentially useful in this respect. The entire, fully corrected data set (70 observations) was used. The parameters so tested were tensile strength, diamond pyramid hardness, engineering strain energy to failure, and true strain energy to failure (corrected for elongation and reduction in area).[28] The resulting predicting equations are arranged in order of decreasing statistical significance in Table 4 along with the correlations previously discussed for ultimate resilience for the fully corrected data set (equation 3) as well as that obtained without NPSH correction (equation 4).

Both of the ultimate resilience equations (3 and 4) are statistically better than any of the others. Tensile strength is reasonably good, hardness considerably worse, and the two strain energies considerably less successful. Note that the engineering strain energy is by far the worst of the group.

VI. COMPARISON OF VENTURI AND VIBRATORY FACILITY RESULTS

A. Predicting Equations. The venturi damage data involves tests in both mercury (70°F) and water (70°F). Since the velocities

TABLE 4

COMPARISON OF PREDICTING EQUATIONS

Mechanical Property	Predicting Equation	CD*	AAPD**	APD***
1. Ultimate Resilience (UR)	Avg. MDP Rate = $0.142 + 8.918(UR)^{-1/2}$	0.780	51.3%	139.0%
Ultimate Resilience (UR)	Avg. MDP Rate = $0.284 + 7.254(UR)^{-1/2} - 0.331(\rho)^{-2}$	0.744	49.5%	164.7%
2. Tensile Strength (TS)	Avg. MDP Rate = $-2.076 + 8.620 \times 10^{2}(TS)^{-1/2}$	0.736	58.9%	133.1%
3. Hardness (H)	Avg. MDP Rate = $6.310 - 0.883(H)^{1/3}$	0.631	63.1%	129.7%
4. True Strain Energy (TSER)	Avg. MDP Rate = $5.136 - 0.119(TSER)^{1/3}$	0.588	77.9%	168.1%
5. Engineering Strain Energy (ESE)	Avg. MDP Rate = $4.602 - 0.132(ESE)^{1/3}$	0.514	326.9%	377.1%

*Coefficient of Determination.

**Average Algebraic Percent Deviation.

***Average Percent Deviation.

were not the same due to facility limitations, the data from the two fluids cannot be considered together. Predicting equations had previously been generated for this data,[6,7] but no generally applicable simple relation was found in terms of the various mechanical properties already mentioned, but excluding ultimate resilience. Since the vibratory data had correlated well in terms of ultimate resilience, the venturi data was also tested for a correlation with this property. It was found that the mercury data could be correlated well in terms of the square root of ultimate resilience (as had the vibratory data), which was, in fact, a better correlation than any other single property correlation previously obtained with this data.[6] However, no significant correlation existed between ultimate resilience and the water data. This may be due to the fact that in the relatively low intensity venturi cavitation field corrosion effects are considerably more important than in the vibratory facility, and probably more important relatively in water than mercury, since the mechanical attack is much more intense with mercury than with water.* The proposed correlating parameter does not in any way consider corrosion.

The resulting correlating equation for the mercury venturi data with relevant statistical information follows:

$$MDP^{**} = 0.034 - 0.879\times10^{-3}(UR)^{1/2} \qquad (5)$$

Coefficient of Determination = 0.878

---

* A correlation of the water-only data from the vibratory facility shows that ultimate resilience is less successful than tensile strength and hardness (Table 7).

** Total mean depth of penetration incurred during test.

B. Relative Material Rankings. Table 5 shows the 70°F mercury data for both facilities, which is the only liquid metal data for which a direct comparison can be made. Venturi damage is given as MDP in 50 hours, and average MDPR is used for the vibratory facility. The materials tested in the two facilities are of similar properties and constituents, but not identical in any of the cases. As an example, T-111 is Ta-8W-2Hf, so these two are of identical composition, whereas T-222 differs slightly in composition from Ta-10W. For both facilities the materials have been listed in order of decreasing cavitation resistance. The first five materials and the last have identical rankings in each facility, while the remaining three differ only slightly in relative ranking between facilities. However, although the relative rankings are quite closely preserved between the two facilities, the factors separating damage in the venturi are several orders of magnitude larger than in the vibratory facility. This may be due to the fact that chemical effects are probably more prominent in the venturi facility.

Table 6 shows a similar comparison of damage in the two facilities for the water tests. There is much less agreement in relative rankings between the facilities than was the case for mercury. Again, this may be due to the relatively prominent role played by chemical effects in the water venturi data.

VII. CONCLUSIONS

A) A cavitation-damage predicting equation, which is sufficiently consistent with the present vibratory facility data for

TABLE 5

COMPARISON OF CAVITATION EROSION DATA IN MERCURY AT 70°F - VENTURI AND ULTRASONIC FACILITIES

Venturi Data		Ultrasonic Data	
Material	MDP at 50 Hours	Material	Avg. MDP Rate
Stainless Steel	$.28 \times 10^{-2}$ mils	304 SS	.32 mils/hr.
		316 SS	.33
Ta-8W-2Hf	$.85 \times 10^{-2}$	T-111	.35
Ta-10W	1.71×10^{-2}	T-222	.43
Mo-1/2Ti	2.10×10^{-2}	Mo-1/2Ti	.57
Carbon Steel	2.94×10^{-2}	Cb-1Zr	.92
Cb-1Zr(A)	5.87×10^{-2}	Carbon Steel	1.03
Cb-1Zr	29.0×10^{-2}	Cb-1Zr(A)	1.61
Plexiglas	225×10^{-2}*	Plexiglas	3.99

*MDP at 25 hours.

TABLE 6

COMPARISON OF CAVITATION EROSION DATA IN WATER AT 70°F
VENTURI AND ULTRASONIC FACILITIES

Venturi Data		Ultrasonic Data	
Material	MDP at 50 Hours	Material	Avg. MDP Rate
Cb-1Zr	3.50×10^{-3} mils	T-222	0.02 mils/hr.
Stainless Steel	5.27×10^{-3}	T-111	0.06
		Mo-1/2Ti	0.09
Ta-8W-2Hf	7.62×10^{-3}	316 SS	0.09
Ta-10W	11.11×10^{-3}	304 SS	0.10
Cb-1Zr(A)	20.29×10^{-3}	Cb-1Zr	0.15
Plexiglas	67.25×10^{-3}*	Cb-1Zr(A)	0.18
Mo-1/2Ti	99.72×10^{-3}	Carbon Steel	0.23
Carbon Steel	769.2×10^{-3}	2024 Al	0.57
2024 Al	1618×10^{-3}	6061 Al	0.72
6061 Al	1976×10^{-3}	Plexiglas	1.39
1100-0 Al	2451×10^{-3}	1100-0 Al	2.70
Cu-Zn	39.77×10^{-3} mils		0.38 mils/hr.
Ni	14.85×10^{-3}		0.44
Cu-Ni--1800°F anneal	8.58×10^{-3}		0.47
Ni-1600°F anneal	4.04×10^{-3}		0.48
Ni-1100°F anneal	14.63×10^{-3}		0.58
Cu-Ni--1300°F anneal	13.29×10^{-3}		0.63
Cu-Zn--1400°F anneal	25.09×10^{-3}		0.68
Cu-Ni	19.23×10^{-3}		0.70
Cu-Zn--850°F anneal	25.72×10^{-3}		0.72
Cu	24.29×10^{-3}		0.95
Cu-1500°F anneal	27.62×10^{-3}		0.95
Cu-900°F anneal	23.75×10^{-3}		1.02

*MDP at 4 hours.

TABLE 7

SUMMARY OF SINGLE PROPERTY CORRELATIONS OF WATER DATA ONLY
(ALL WATER DATA)

No dependence on fluid properties since only one fluid-temperature combination involved.

Property	Predicting Equation	CD**
1. Tensile Strength (TS)	$MDPR^{*}=-1.570 + 6.84\times10^{2}(TS)^{-\frac{1}{2}}$	0.851
2. Hardness (H)	$MDPR = -0.267 + 16.62(H)^{-\frac{1}{2}}$	0.754
3. Ultimate Resilience (UR)	$MDPR = 0.591 + 8.504(UR)^{-\frac{1}{2}}$	0.673
4. Engineering Strain Energy (ESE)	$MDPR = 0.036 + 29.99(ESE)^{-1/3}$	0.624
5. True Strain Energy (TSER) (Corrected for elongation and reduction in area)	$MDPR = 3.557 - 6.55\times10^{-2}(TSER)^{1/3}$	0.607

* Average mean depth of penetration rate.

**Coefficient of Determination.

engineering estimates, and which is relatively simple in form, has been found. The data used in determining this equation was obtained in vibratory cavitation damage tests in water, mercury, lithium, and lead-bismuth alloy, with an extreme temperature range for the latter two between 500°F and 1500°F. The materials tested include a very wide spectrum of metals, including some refractory alloys. The predicting equation follows:

$$MDPR = C_1 \cdot C_2[0.142 + 8.918(UR)^{-1/2}]$$

An alternate equation, which is nearly as good statistically, is:

$$MDPR = C_2[0.284 + 7.254(UR)^{-1/2} - 0.331(\rho)^{-2}]$$

B) Damage correction factors for the cavitation "thermodynamic effect" and for variable static NPSH used in the vibratory test have been derived and evaluated for use in the above predicting equations.

C) It was found that ultimate resilience was by far the most successful single material property for predicting cavitation damage. The other properties which were investigated, listed in decreasing order of success, were tensile strength, diamond pyramid hardness, "true" strain energy, and finally, "engineering" strain energy.

D) Relative rankings of different materials based on damage obtained in the vibratory facility and in our venturi facility were almost identical for mercury (the only liquid metal used in the venturi). Also, a predicting equation in terms of ultimate resilience, quite similar to that found for the vibratory data, applied also to the mercury

venturi data. However, the relative rankings of materials tested in water in the two facilities differed widely, and no correlation with ultimate resilience was found for the water venturi data. It is believed that these discrepancies in the case of water are due to the relatively large role presumably played by chemical effects in the low intensity water venturi cavitation field.

REFERENCES

1. Garcia, R. and Hammitt, F. G., "Ultrasonic-Induced Cavitation in Liquid Metals at 1500°F," Internal Report No. 05031-1-I, Department of Nuclear Engineering, The University of Michigan, February, 1965; also Transactions of the American Nuclear Society, 8, 1, June, 1965, pp. 18-19.

2. Garcia, R. and Hammitt, F. G., "Ultrasonic-Induced Cavitation Studies in Lead-Bismuth Alloy, 500-1500°F," Corrosion, 22, 6, June, 1966, pp. 157-167.

3. Garcia, R., Hammitt, F. G. and Nystrom, R. E., "Comprehensive Cavitation Damage Data for Water, Mercury, and Lead-Bismuth Alloy Including Correlations with Material and Fluid Properties," ORA Technical Report No. 05031-4-T, Department of Nuclear Engineering, The University of Michigan, May, 1966; presented at ASTM Annual Meeting, Symposium on Erosion by Cavitation or Impingement, Atlantic City, New Jersey, June, 1966; to be published by ASTM.

4. Garcia, R., "Comprehensive Cavitation Damage Data for Water and Various Liquid Metals Including Correlations with Material and Fluid Properties," Ph.D. Thesis and ORA Technical Report No. 05031-6-T, Department of Nuclear Engineering, The University of Michigan, August, 1966.

5. Hammitt, F. G., "Cavitation Damage and Performance Research Facilities," Symposium on Cavitation Research Facilities and Techniques, pp. 175-184, ASME Fluids Engineering Division, May, 1964. See also ORA Technical Report No. 03424-12-T, Department of Nuclear Engineering, The University of Michigan, November, 1963.

6. Robinson, M. John, "On the Detailed Flow Structure and the Corresponding Damage to Test Specimens in a Cavitating Venturi," Ph.D. Thesis and ORA Technical Report No. 03424-16-T, Department of Nuclear Engineering, The University of Michigan, August, 1965.

7. Robinson, M. J. and Hammitt, F. G., "Detailed Damage Characteristics in a Cavitating Venturi," ORA Internal Report No. 03424-30-I, Department of Nuclear Engineering, The University of Michigan, June, 1966; to be published J. Basic Eng. Trans. ASME.

8. Garcia, R. and Hammitt, F. G., "Amplitude Determination of an Ultrasonic Transducer by Means of an Accelerometer Assembly," ORA Internal Report No. 05031-7-I, Department of Nuclear Engineering, The University of Michigan, December, 1965.

9. Jackson, F. J. and Nyborg, W. L., "Sonically-Induced Microstreaming Near a Plane Boundary. I. The Sonic Generator and Associated Acoustic Field," J. of the Acoustical Society of America, 32, 10, October, 1960, pp. 1243-1250.

10. Jackson, F. J., "Sonically-Induced Microstreaming Near a Plane Boundary. II. Acoustic Streaming Field," J. of the Acoustical Society of America, 32, 11, November, 1960, pp. 1387-1395.

11. Crofford, W. N., Kovacina, T. A. and Miller, R. R., "Isothermal Study of Concentration and Transport of Radioactive Stainless Steel Components in Liquid Lithium," NRL Report 5572, U.S. Dept. of Commerce, Dec. 29, 1960.

12. Plesset, M. S., "The Pulsation Method for Generating Cavitation Damage," J. Basic Eng. Trans. ASME, 85, Series D, No. 3, 1963, pp. 360-364. See also "Pulsing Technique for Studying Cavitation Erosion of Metals," Corrosion, 18, 5, May, 1962, pp. 181-188.

13. Stahl, H. A. and Stepanoff, A. J., "Thermodynamic Aspects of Cavitation in Centrifugal Pumps," Trans. ASME, 78, 1956, pp. 1691-1693.

14. Hammitt, F. G., "Liquid-Metal Cavitation--Problems and Desired Research," ASME Paper No. 60-HYD-13, March, 1960.

15. Nowotny, H., "Destruction of Materials by Cavitation," VDI-Verlag, Berlin, Germany, 1942. Reprinted by Edwards Brothers, Inc., Ann Arbor, Michigan, 1946. English Translation available as ORA Internal Report No. 03424-15-I, Department of Nuclear Engineering, The University of Michigan, 1962.

16. Leith, W. C. and Thompson, A. Lloyd, "Some Corrosion Effects in Accelerated Cavitation Damage," ASME Paper No. 59-A-52, November, 1959.

17. Devine, R. E. and Plesset, M. S., "Temperature Effects in Cavitation Damage," Report No. 85-27, Division of Engineering and Applied Science, California Institute of Technology, Pasadena, California, April, 1964.

18. Hobbs, J. M., "Experience with a 20-Kc. Cavitation Erosion Test," Paper #120 presented at 1966 Annual ASTM Meeting, Symposium on Erosion by Cavitation or Impingement, Atlantic City, New Jersey, June, 1966.

19. Kemppainen, D. J. and Hammitt, F. G., "Effect of Temperature on Cavitation Damage," ORA Internal Report No. 05031-10-I, Department of Nuclear Engineering, The University of Michigan, July, 1966.

20. Thiruvengadam, A., Preiser, H. S. and Rudy, S. L., "Cavitation Damage in Liquid Metals," Technical Progress Report 467-2 (NASA CR-54391) For the Period January 1, 1965 to March 31, 1965, Hydronautics, Inc., April 28, 1965.

21. Thiruvengadam, A., Preiser, H. S. and Rudy, S. L., "Cavitation Damage in Liquid Metals," Technical Progress Report 467-3 (NASA CR-54459) For the Period April 1, 1965 to May 31, 1965, Hydronautics, Inc., June 30, 1965.

22. Leith, W. C., "Prediction of Cavitation Damage in the Alkali Liquid Metals," Proceedings ASTM, 65, 1965, pp. 789-800.

23. Florschuetz, L. W. and Chao, B. T., "On the Mechanics of Vapor Bubble Collapse--A Theoretical and Experimental Investigation," Report ME-TN-1069-2, Department of Mechanical and Industrial Engineering, The University of Illinois, Urbana, Illinois, October, 1963.

24. Collier, J. G., "The Boiling of Sodium and Its Significance to the Safety of Fast Reactors," Internal Document, Chemical Engineering Division, A.E.R.E. Harwell, January, 1966.

25. Plesset, M. S. and Zwick, S. A., "The Growth of Vapor Bubbles in Superheated Liquids," J. of Applied Physics, 25, 4, April, 1954, pp. 493-500.

26. Westervelt, Franklin H., "Automatic System Simulation Programming," Ph.D. Thesis, College of Engineering, The University of Michigan, November, 1960.

27. Crandall, Richard L., "The Mathematical and Logical Procedures of the Stepwise Regression Program with Learning," University of Michigan Computing Center Internal Report, 1965.

28. Harrison, Curtis A., Robinson, M. John, Siebert, Clarence A., Hammitt, Frederick G. and Lawrence, Joe, "Complete Mechanical Properties Specifications for Materials as Used in Venturi Cavitation Damage Tests," ORA Internal Report No. 03424-29-I, Department of Nuclear Engineering, The University of Michigan, August, 1965.